Seeing faces is necessary for face-domain formation

Michael J Arcaro[1,2], Peter F Schade[1,2], Justin L Vincent[1], Carlos R Ponce[1] & Margaret S Livingstone[1,2]

Here we report that monkeys raised without exposure to faces did not develop face domains, but did develop domains for other categories and did show normal retinotopic organization, indicating that early face deprivation leads to a highly selective cortical processing deficit. Therefore, experience must be necessary for the formation (or maintenance) of face domains. Gaze tracking revealed that control monkeys looked preferentially at faces, even at ages prior to the emergence of face domains, but face-deprived monkeys did not, indicating that face looking is not innate. A retinotopic organization is present throughout the visual system at birth, so selective early viewing behavior could bias category-specific visual responses toward particular retinotopic representations, thereby leading to domain formation in stereotyped locations in inferotemporal cortex, without requiring category-specific templates or biases. Thus, we propose that environmental importance influences viewing behavior, viewing behavior drives neuronal activity, and neuronal activity sculpts domain formation.

How do we develop the brain circuitry that enables us to recognize a face? In humans and in monkeys, inferotemporal cortex (IT) is subdivided into domains that selectively process different image categories, such as faces, bodies, or scenes. The biological importance of faces for social primates and the stereotyped locations of face-selective domains in both humans and monkeys have engendered the idea that face domains are innate neural structures[1,2]. The view that face processing is carried out by an innate, specialized circuitry is further supported by preferential looking at faces very early on by human[3,4] and non-human primate infants[5] (see, however, refs. 6,7), and by the fact that faces, more so than other image categories, are recognized most proficiently as upright, intact wholes[8,9]. However, genetic specification of something as particular as a face template, or even a response bias for such a high-level category, in IT seems inconsistent with the widely accepted view that the visual system is wired up by activity-dependent self-organizing mechanisms[10]. Furthermore, the existence of IT domains for unnatural object categories, such as text[11] and buildings[12], and the induction of highly unnatural symbol domains in monkeys by training[13], all indicate a major effect of experience on IT domain formation. Yet, as pointed out by Malach and colleagues[14,15], both biological and unnatural domains invariably occur in stereotyped locations, and this consistency mandates some kind of proto-architecture. The mystery is what kind of innate organization could be so modifiable by experience as to permit the formation of domains for such unnatural categories as buildings[12], tools[16], chairs[17], or text[11] yet result in stereotyped neuroanatomical locations for these domains. Here we show that lack of early visual experience of faces leads to the absence of face-selective domains but not of other category-selective domains. Furthermore, we show that preferential face-looking behavior precedes the emergence of face domains in monkeys raised with normal face experience. We recently reported that a strong retinotopic proto-organization is present throughout the visual system in newborn macaques, well before the emergence of category domains in IT[18]. Therefore, the selectivities and stereotyped locations of category domains could be a consequence of viewing behavior that determines where activity-dependent changes occur on this retinotopic proto-map.

RESULTS

Face patches in control and face-deprived monkeys

To find out whether seeing faces is necessary for acquiring face domains, we raised three macaques without any visual experience of faces. These monkeys were hand-reared by humans wearing welder's masks. We took extensive care to handle and play with the monkeys several times every day, and we provided fur-covered surrogates that hung from the cage and moved in response to the monkey's activity. We also provided them with colorful interactive toys and soft towels that were changed frequently so these monkeys had an otherwise responsive and visually complex environment. These kinds of early interventions have been shown to prevent depression and support normal socialization[19]. The face-deprived monkeys were kept in a curtained-off part of a larger monkey room so they could hear and smell other monkeys. They were psychologically assessed during the deprivation period and were consistently found to be lively, curious, exploratory, and interactive. The face-deprived monkeys were introduced to social housing after the deprivation period and have all integrated normally into juvenile social groups.

We scanned control and face-deprived monkeys while they viewed images of different categories (**Supplementary Fig. 1**). We recently reported that, in typically reared macaques, face domains (i.e., patches or regions in the superior temporal sulcus (STS) that are selectively responsive to faces) are not present at birth but instead emerge gradually over the first 5–6 months of life[20]. By 200 days of age, all the control monkeys showed robust, stereotyped patches more responsive to faces than objects (faces>objects) that were remarkably stable across sessions (ref. 20 and **Fig. 1**). The control monkeys consistently showed significant faces>objects activations in four or

[1]Department of Neurobiology, Harvard Medical School, Boston, Massachusetts, USA. [2]These authors contributed equally to this work. Correspondence should be addressed to M.S.L. (mlivingstone@hms.harvard.edu).

five patches distributed along the lower lip and fundus of the STS, as previously described in adult monkeys[21]. The face-deprived monkeys, in contrast, consistently showed weak, variable, or no significant faces>objects activations in either the expected locations along the STS or anywhere else. The reproducibility of the face patches in control monkeys across sessions, and the impressive difference in face activations between control and face-deprived monkeys, are clear from the individual session maps in **Figure 1**.

To quantify the consistency across scan sessions, we correlated the beta contrast maps for faces-minus-objects within an anatomically defined region of interest (ROI) that consisted of the STS and its lower lip (black dotted outline on B4 map in **Fig. 1**). The spatial pattern of (unthresholded) beta values within the STS ROI for faces-minus-objects was highly reproducible across sessions for both control monkeys (mean $r = 0.86 \pm 0.02$ s.e.m.) and face-deprived monkeys (mean $r = 0.66 \pm 0.02$ s.e.m.) (see **Supplementary Table 1** for information on individual monkeys). However, removing object-selective voxels from the analysis almost entirely eliminated any cross-session correlation in the face-deprived monkeys (mean $r = 0.02 \pm 0.06$ s.e.m.), suggesting that the consistency of the beta map pattern of faces-minus-objects was driven by object-selective responsiveness, and therefore there was no consistency to the face-selective responsiveness in the face-deprived monkeys. In contrast, faces-minus-objects correlations remained strong in the control monkeys, even when the object-selective voxels were removed from the analysis (mean $r = 0.72 \pm 0.05$ s.e.m.). This analysis further demonstrates that the spatial pattern of face-selective activity was consistent across sessions for the control monkeys, but inconsistent across sessions for face-deprived monkeys. Conjunction maps (**Fig. 2**) further demonstrate this reproducibility by illustrating spatially consistent activity across sessions for all the monkeys that were scanned in multiple sessions. Taken together, these data demonstrate a marked difference between control and face-deprived monkeys, specifically in face-selective responsiveness in IT.

Hand>object patches in control and face-deprived monkeys

The unexpected result that face-deprived monkeys had weak or no face selectivity in the STS or anywhere else motivated us to examine other domains that normally occur in IT. In most monkeys, body domains are adjacent to, and partially overlapping with, face patches[21,22]. Reasoning that the most often seen, and behaviorally significant, body part for the hand-reared face-deprived monkeys would be their own hands, or the gloved hands of laboratory staff, we scanned the monkeys while they viewed interleaved blocks of monkey hands or gloved human hands along with blocks of faces and blocks of objects. All the face-deprived monkeys showed strong hand activations in roughly the same fundal regions of the STS as control monkeys (**Figs. 1** and **2**). The spatial pattern of (unthresholded) beta values within the STS ROI for hands-minus-objects was reproducible across sessions for both control monkeys (mean $r = 0.49 \pm 0.07$ s.e.m.) and face-deprived monkeys (mean $r = 0.76 \pm 0.01$ s.e.m.) (see **Supplementary Table 1** for information on individual monkeys). Furthermore, cross-session correlations remained strong for both control and face-deprived monkeys even when object-selective voxels were removed from the analysis (mean $r = 0.26 \pm 0.05$ s.e.m. and 0.65 ± 0.03 s.e.m., respectively), demonstrating that the locations of hand-selective responses in the STS were stable across scans. **Figures 1** and **2** show that, in face-deprived monkeys, the hands>objects patches were stronger, larger, and more anatomically consistent across sessions than the sparse faces>objects activations, whereas, in control monkeys, the hand patches were smaller or equivalent in size to the face patches.

### Hand>object versus face>object patches in control and face-deprived monkeys

The sizes of the face and hand patches differed between control and face-deprived monkeys. **Figure 2b** quantifies these differences between control and face-deprived monkeys in an entire-STS ROI (ROI is shown as a dotted outline in the B4 map in **Fig. 2a**). **Figure 2b** compares, in each monkey, the number of 1-mm^3 voxels in this ROI that were significantly more activated by faces than by objects with the number of hands>objects voxels (voxels selected using $P < 0.01$ FDR corrected threshold). The number of hand-selective voxels in the STS ROI was larger than the number of face-selective voxels for every scan session in each face-deprived monkey. This difference was significant for every face-deprived monkey (two-tailed, paired-sample t-test across sessions and across hemispheres; B6, $t(17) = -13.5$, $P = 2 \times 10^{-10}$; B9, $t(17) = -8.2$, $P = 3 \times 10^{-7}$; B10, $t(11) = -6.7$, $P = 3 \times 10^{-5}$). The opposite held true for two control monkeys, in that there were significantly more face-selective voxels than hand-selective voxels (B4: $t(5) = 3.2$; $P = 0.02$; B8: $t(5) = 6.4$; $P = 0.001$), and in the third control monkey, B5, there was no significant difference between the number of face-selective voxels and the number of hand voxels ($t(5) = -1.0$; $P = 0.4$). Although our sample size was too small for robust group-level comparisons, fixed-effects analyses converged with the within-subject analyses ("Group-level, fixed-effects analyses" subsection in Online Methods). Furthermore, the smaller number of face-selective voxels in the face-deprived monkeys cannot be attributed to an overall diminished responsiveness in the STS, because the average number of hand-selective voxels was actually larger in face-deprived monkeys than in control monkeys (311 versus 202 voxels on average). These analyses confirmed the impression from the beta contrast maps in **Figures 1** and **2** that control monkeys showed more face-selective activation in the STS than did face-deprived monkeys, and demonstrate a specific deficit of face-selective, but not hand-selective, activity in the face-deprived monkeys.

Fixation during scanning

Can any artifact in our study design explain the selective deficit in face responsiveness in IT of face-deprived monkeys? Analysis of responsiveness in primary visual cortex (V1) (**Fig. 2c**) and fixation behavior during scanning (**Supplementary Fig. 2**) indicated that there were no differences in fixation behavior during scanning that could explain the large differences between control and face-deprived monkeys in face-selective activations ("Fixation during scanning" subsection in Online Methods).
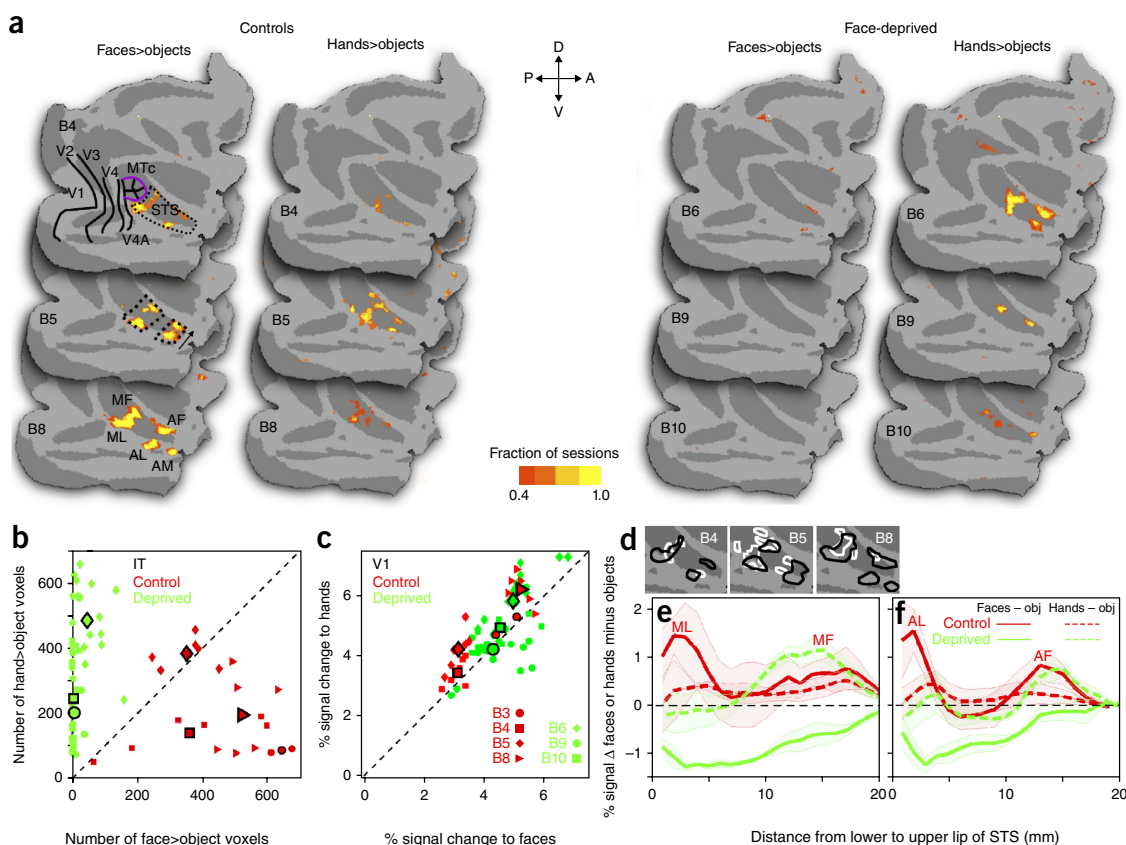
Relative locations of face and hand activations

Because face-deprived monkeys had slightly larger hand patches than control monkeys, we wondered whether this indicated a takeover of face territory by hand responsiveness. As can be seen in **Figures 1** and **2**, the face and hand patches overlapped, but the hand patches were centered slightly deeper in the sulcus compared to the face patches (**Fig. 2d**). To measure the locations of the face and hand activations along the depth of the STS, we drew two other anatomically defined ROIs, one in central IT (CIT) and another in anterior IT (AIT). These ROIs spanned from the lower lip through the STS fundus to the upper bank and thus encompassed (in control monkeys) the face patches on the lower lip of the STS (ML/AL[21,22]) and in the fundus (MF/AF[21,22]) in CIT and AIT (ROIs are shown by the dotted lines in the B5 face map in **Fig. 2a**). We drew these ROIs to maximally sample the face patches in control monkeys and the hand patches in all the monkeys, to compare in control and face-deprived monkeys the relative mediolateral locations of face and hand responsiveness with respect to the anatomical landmarks, banks, and fundus of the STS. The beta coefficients for
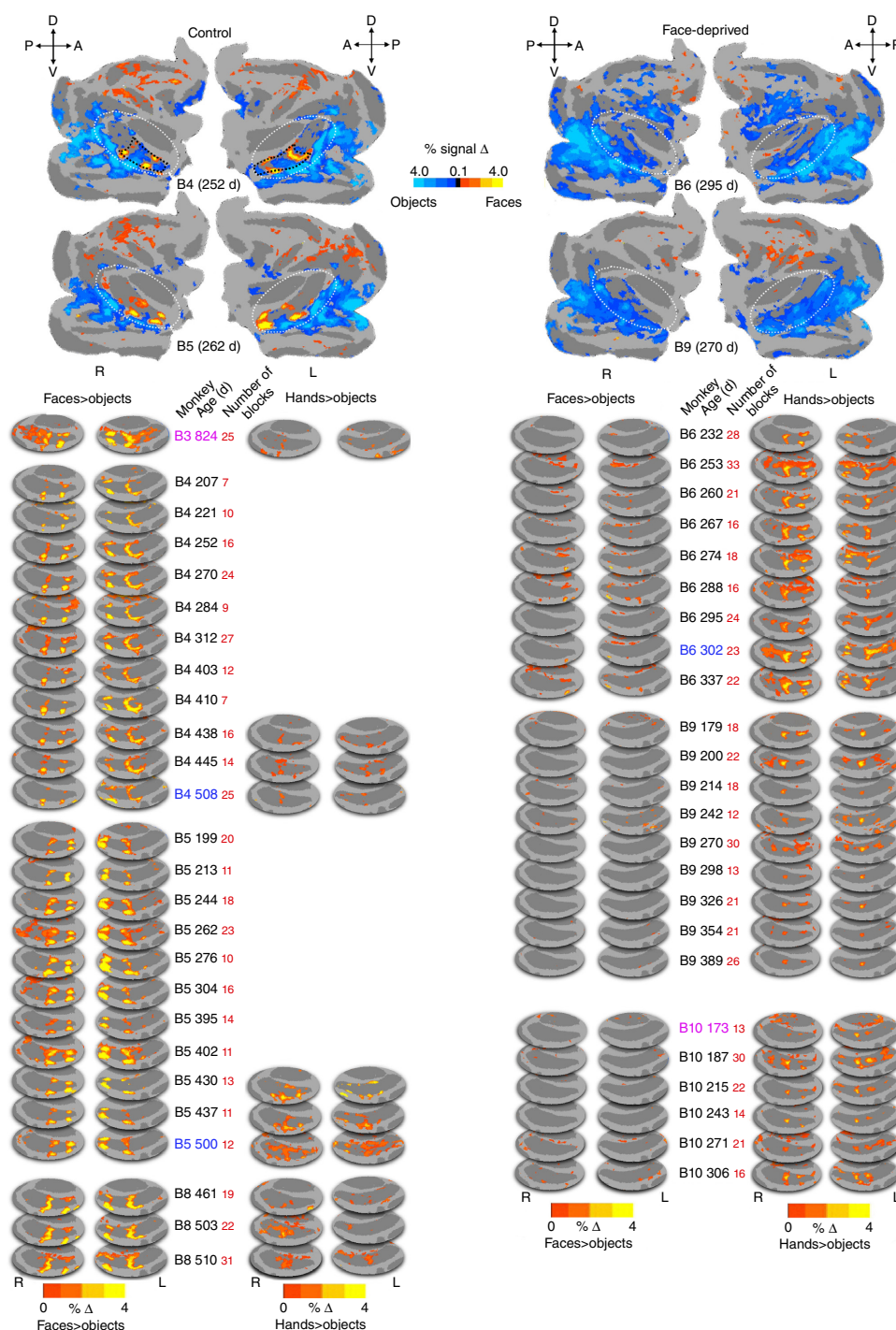
Figure 1 Faces>objects and hands>objects activations in control and face-deprived monkeys. Top, representative maps for the contrast faces-minus-objects aligned onto the standard macaque F99 flattened cortical surface (light gray, gyri; dark gray, sulci). These examples show percent signal change (beta coefficients) thresholded at $P < 0.01$ (FDR corrected) for one session each for two control (B4 and B5; left) and two face-deprived (B6 and B9; right) monkeys at 252, 262, 295, and 270 days old, as indicated. Dotted white ovals indicate the STS region shown in the bottom half for all scan sessions for all seven monkeys. Dotted black outline in B4 map shows the STS ROI used for the correlation analysis described in the text. Bottom, faces>objects and hands>objects beta maps, thresholded at $P < 0.01$ (FDR-corrected), for all individual scan sessions at the ages (in days) indicated for four control monkeys (B3, B4, B5 and B8; left) and three face-deprived monkeys (B6, B9 and B10; right). For all but the five scan sessions indicated by colored lettering, the images were single large monkey faces, monkey hands, or objects (**Supplementary Fig. 1**). For the scan sessions B4 508, B5 500, and B6 302, the hands were gloved human hands; for scan sessions B3 824 and B10 173, the stimuli were mosaics of monkey faces, monkey hands, or objects, rather than single large images (these were sessions in which scenes were also presented, and mosaics were used to equate visual-field coverage). The small red numbers indicate the number of blocks of each category type included in the analysis for each session. D, dorsal; V, ventral; A, anterior; P, posterior.

Figure 2 Quantification of face and hand activations in control and face-deprived monkeys. (**a**) Conjunction analysis: flat maps show the proportion of sessions for each monkey (that was scanned in multiple sessions) for which each voxel was significantly more activated by faces>objects or by hands>objects for three control monkeys (left) and three face-deprived monkeys (right). Significance threshold for each session was $P < 0.01$ (FDR-corrected). The five previously described face patches typically found in control monkeys are labeled in the B8 face map[21,22]. Across sessions, face patch AM was consistently significant in only monkey B8, although it was present at subthreshold levels in monkeys B4 and B5. In monkey B4, areal borders between V1, V2, V3, V4, and V4A are indicated in black, and the MT cluster is outlined in purple; areas were determined by retinotopic mapping at 2 years of age in the same monkey. (**b**) Number of voxels in an anatomically defined entire-STS ROI (outlined in B4 face map) that were significantly more activated by faces than by objects (horizontal axis) compared to the number of voxels in the same ROI that were significantly more activated by hands than by objects (vertical axis). Voxels selected at $P < 0.01$ FDR-corrected threshold. Different symbols represent different monkeys, and each symbol represents data from one hemisphere from one scan session for one control (red) or one face-deprived (green) monkey. Large symbols with black outlines show means for each monkey across sessions and hemispheres (for B3, only across hemispheres). (**c**) Percent signal change in a central V1 ROI (central 6–7° of visual field) in response to faces (horizontal axis) or hands (vertical axis). Each symbol represents data from one hemisphere for one scan session for one monkey; large symbols show means for each monkey that was scanned multiple times; single-session mean across hemispheres for B3 is highlighted in black. (**d**) Overlays of face (black) and hand (white) patches for each of the control monkeys from the conjunction analysis. (**e**) Average percent signal change (s.e.m. indicated by shading) to faces minus objects (solid lines) and hands minus objects (dashed lines) as a function of ventrolateral to dorsomedial distance along an anatomically defined CIT ROI that extends from the crown of the lower lip of the STS to the upper bank of the STS (leftmost outlined region on the B5 face map; arrow on map corresponds to x axis on graph). Data were averaged over all sessions and both hemispheres of all three control monkeys that were scanned multiple times (red lines) and all three face-deprived monkeys (green lines). Activations were averaged across the anterior–posterior dimension of the ROI to yield an average response as a function of mediolateral location. (**f**) Same as **e**, except for an anatomically defined AIT ROI (right outlined region on the B5 face map).

faces-minus-objects (solid lines) and hands-minus-objects (dotted lines) were averaged across the anterior–posterior (AP) dimension of the CIT ROI (**Fig. 2e**) and the AIT ROI (**Fig. 2f**) for all the control (red) and face-deprived (green) monkeys. On average, face-deprived monkeys showed enhanced hands-minus-objects responses (green dashed lines) in the fundus of the STS. **Supplementary Figure 3** shows the raw percent signal change to faces, hands, and objects for the same CIT and AIT ROIs, from which it can be determined that these regions in face-deprived monkeys do respond to faces, just less than to hands or objects. Since the peak hand selectivity in face-deprived monkeys was maximal in the depth of the STS, it seems likely that the hand activations in the fundus

of the STS in the face-deprived monkeys represent hand responsiveness in what would normally be hand patches, rather than takeover by hands of what would normally be face territory. Nevertheless, our results are not inconsistent with the idea that hand and face selectivities compete for cortical territory.

Scene and body patches in control and face-deprived monkeys
Because the face-deprived monkeys' face-patch organization was grossly abnormal and they showed strong hand selectivity, we wondered about other IT domains. Therefore, we conducted scan sessions contrasting blocks of scenes with faceless bodies and found that
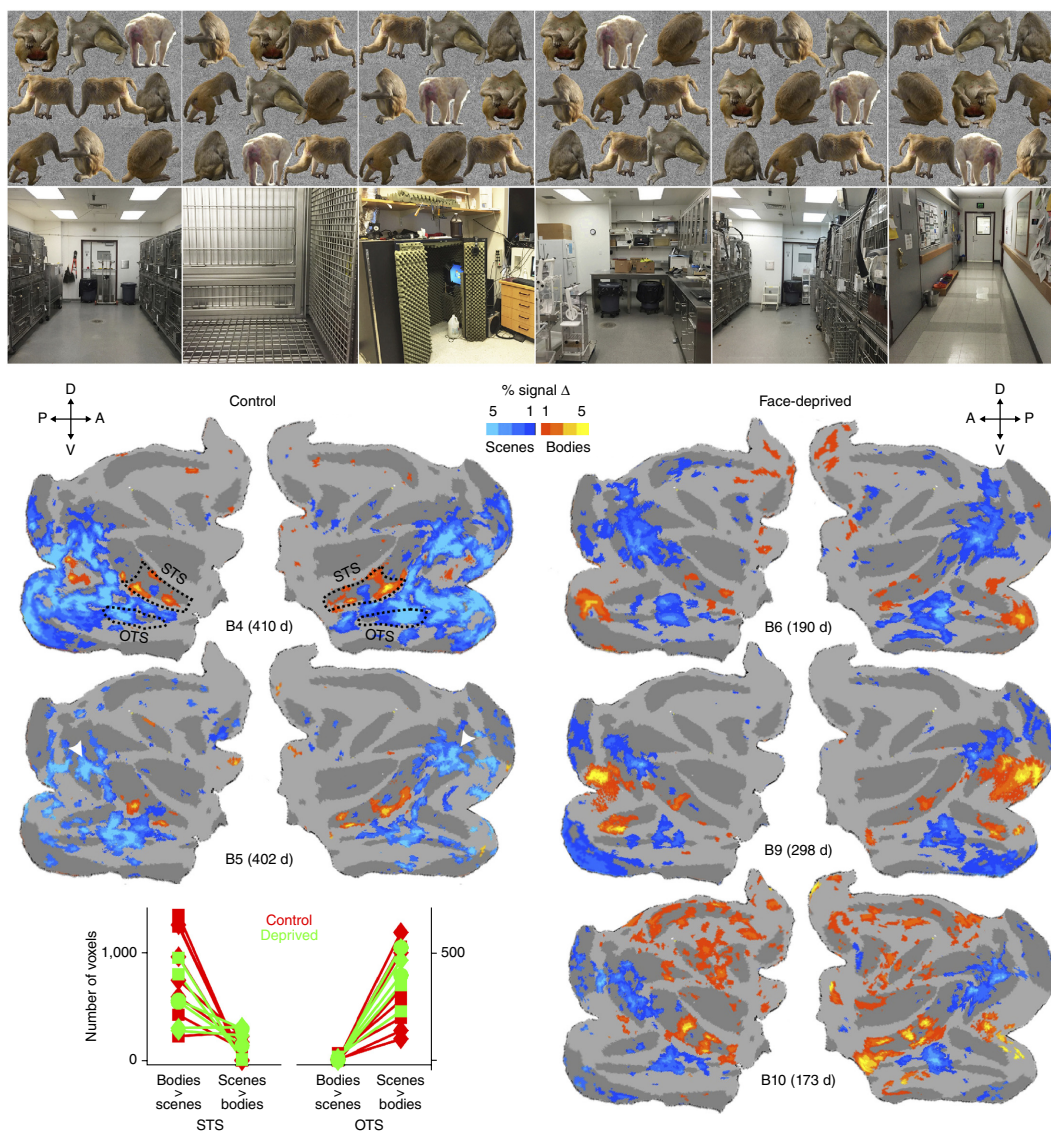
Figure 3 Activations to bodies minus scenes. Top, subset of the images used for bodies-versus-scenes scans. Bottom, maps (beta values) for bodies minus scenes, thresholded at $P < 0.01$ (FDR-corrected), for two control monkeys and three face-deprived monkeys at the ages indicated. The two control monkeys were scanned in an additional session and showed similar activation patterns (B4 326 and B5 318). The graph shows the number of voxels in each monkey in each session in each hemisphere in each ROI (outlined in the B4 maps) that were significantly more responsive to bodies than to scenes, or the reverse, as indicated (voxels selected at a $P < 0.01$ FDR-corrected threshold). Each symbol corresponds to one monkey; red symbols indicate control monkeys, and green symbols indicate face-deprived monkeys.

face-deprived monkeys showed scene and body patches in roughly the same locations as did control monkeys (**Fig. 3**). All the monkeys showed bodies>scenes activations lying along the STS, as well as two regions of scenes>bodies activations, one in the occipitotemporal sulcus (OTS; outlined in the B4 map in **Fig. 3**), which corresponds to the lateral place patch (LPP)[23,24], a potential homologue of the human parahippocampal place area (PPA)[24], and one more dorsally in dorsal prelunate cortex, a region that corresponds to the 'dorsal scene patch'[25], the potential homologue of the human scene area in the transverse occipital sulcus (TOS) (indicated by white arrowheads in the B5 map in **Fig. 3**). Because the STS and the OTS are clear anatomical regions (the dorsal scene patch did not have any clear anatomical ROI that did not also include early visual areas), we used two anatomically defined ROIs to compare scene and body

activations—one, the same STS ROI that we used to quantify face-and-hand activations (outlined on the B4 map in **Fig. 3**), and the other, an OTS ROI drawn to encompass the entire OTS and its ventral lip, which is also outlined on the same map. **Figure 3** compares the number of significant bodies>scenes voxels and the number of scenes>bodies voxels (voxels selected at $P < 0.01$ FDR-corrected threshold) in each ROI in each hemisphere in each monkey for all bodies-versus-scenes scan sessions (**Fig. 3**). Group-level comparisons converged with these individual subject scenes-versus-bodies contrast maps ("Group-level fixed-effects analyses" subsection in the Online Methods). Thus, both control and deprived monkeys showed a similar pattern of selectivity for bodies in the STS and for scenes in the OTS. These complementary patterns of activation to scenes and bodies, as well as the pattern of hand activation in the STS, in the deprived
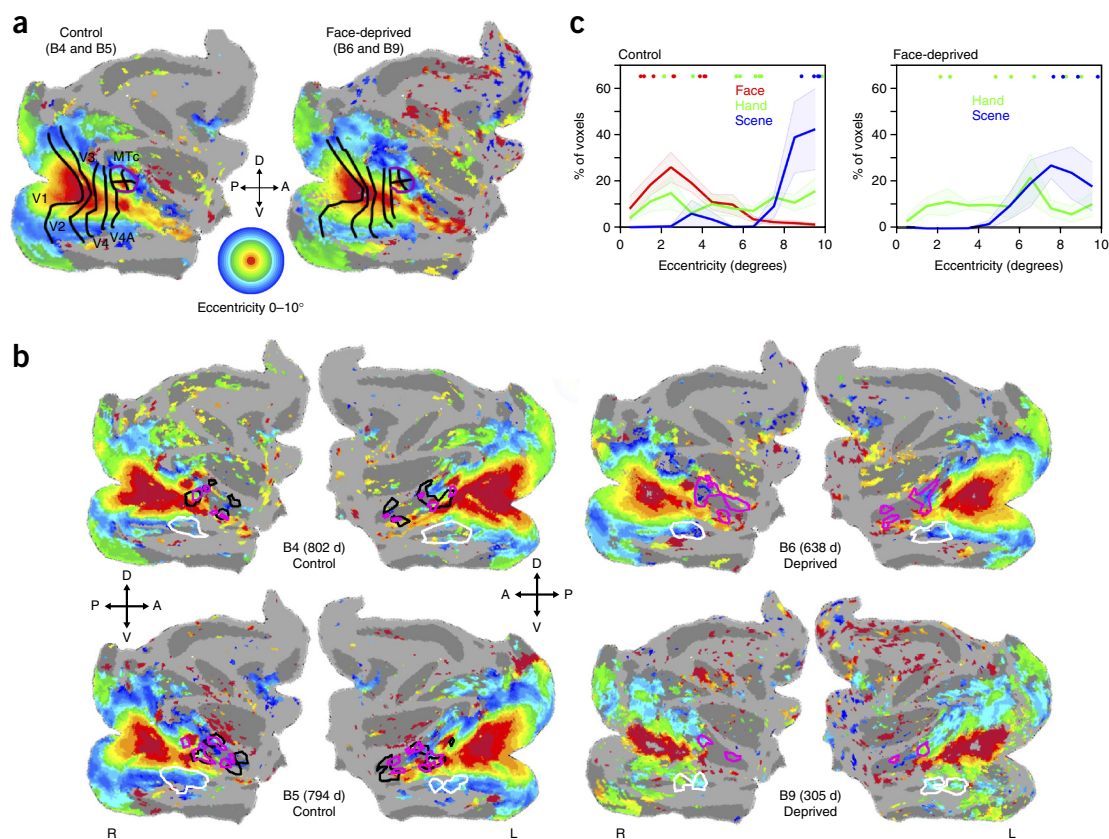
Figure 4 Eccentricity organization in control and face-deprived monkeys. Eccentricity, from 0° (red) to 10° (blue), as indicated by the circular color scale, was mapped using expanding and contracting annuli of flickering checkerboard patterns. (**a**) Average eccentricity organization for two control monkeys (B4 and B5) (left) and two face-deprived monkeys (B6 and B9) (right). Thick black lines indicate areal borders of (left to right) V1, V2, V3, V4, and V4A, and the purple outline indicates the MT cluster, comprising areas MT, MST, FST, and V4t. Across 19 retinotopic areas[26–28], the mean voxel-wise distance between eccentricity maps for the control and face-deprived monkeys was 0.9° ± 1° s.d. The correlation (*r*) between averaged maps for control and face-deprived monkeys was 0.82. Even considering only IT cortical areas, the mean difference between averaged maps for control and face-deprived monkeys was 1.4° ± 1.5° s.d., with a correlation of 0.66, which is comparable to the consistency between individual control monkeys (1.84° ± 1.76° s.d.; correlation = 0.54). (**b**) Individual maps for each hemisphere for each monkey, thresholded at *P* < 0.01. Outlines of the conjunction ROIs for faces (black), hands (magenta), and the ventral scene area (white) for each hemisphere in each monkey are overlaid on each monkey's own eccentricity map. The eccentricity map for monkey B9 is less clear than those of the older monkeys because younger monkeys do not fixate as well, or for as long, as older monkeys. (**c**) Histograms of eccentricity representations (1° bins) within each category-selective ROI averaged across hemispheres for control and face-deprived monkeys. Shading indicates s.e.m. Dots above the graphs indicate the mapped eccentricity of the most category-selective voxel in each face-, hand-, or scene-selective ROI for each hemisphere for each monkey for CIT patches and AIT patches (color indicates ROI category).

monkeys indicated that their IT was organized into at least several non-face category-selective domains.

Eccentricity organization in control and face-deprived monkeys

The face-deprived monkeys not only had hand, body, and scene patches, but the retinotopic organization of their entire visual system was also normal, even in regions of IT that represent faces in control monkeys. **Figure 4** (top) shows average eccentricity maps from phase-encoded retinotopic mapping for two control monkeys (left) and two face-deprived monkeys (right). All the monkeys showed a normal adult-like eccentricity organization across the entire visual system, including IT, with a foveal bias lying along the lower lip of the STS, flanked dorsally and ventrally by more peripheral representations, consistent with previous retinotopic mapping in adult macaques[26–28]. Both control and face-deprived monkeys also showed a separate eccentricity map in posterior fundal STS (**Fig. 4**), corresponding to the MT cluster[26,28]. The lateral face patches ML and AL in control monkeys (ventral black outlines) were located in the strip of foveal bias that lies along the lower lip of the STS[18], as previously reported for adult monkeys[27,29], whereas the fundal

patches MF and AF (dorsal black outlines) lay in more midfield-biased regions. Both control and face-deprived monkeys showed some hand responsiveness (magenta outlines in **Fig. 4b**) in the foveally biased lip of the STS but greater hand responsiveness in the depth of the sulcus, which is more mid visual field. In both control and face-deprived monkeys, scene selectivity (white outlines) mapped to peripherally biased regions of IT, also consistent with previous results in adult monkeys[29]. To illustrate the visual-field biases in these category-selective regions, we plotted the distribution of eccentricity representations of the face, hand, and scene ROIs determined by conjunction analysis (**Fig. 4c**). In control monkeys (**Fig. 4c**, left), face patches were foveally biased, hand patches covered both central and peripheral visual space, and scene patches were peripherally biased. In face-deprived monkeys (**Fig. 4c**, right), visual-field coverage for hand and scene patches was similar to that in controls. Analysis of the eccentricity representation at the most category-selective voxel for each ROI in each monkey showed similar visual field biases as the distribution analysis (**Fig. 4c**; dots at the tops of the graphs). Thus retinotopy, body patches, hand patches, and scene selectivity were not detectably abnormal in face-deprived monkeys, but face selectivity was
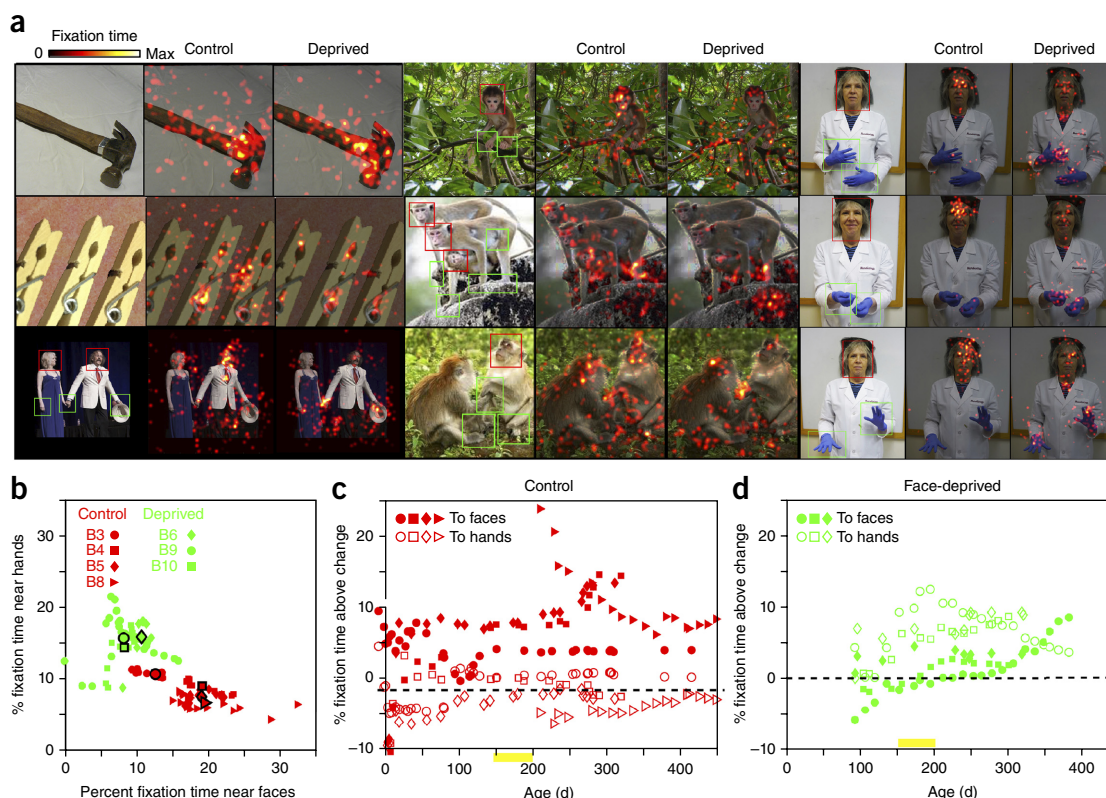
Figure 5 Looking behavior of control and face-deprived monkeys. (**a**) Normalized heat maps of fixations for nine of the images that the monkeys freely viewed while their gaze was monitored. In the leftmost panel for each face-and-hand image, red boxes outline the face regions, and green boxes highlight the hand regions used for the analyses in **b**–**d**. Heat maps combine data from four control and three face-deprived monkeys overlaid onto a darkened version of the image viewed (left bottom photograph by A. Stubbs, courtesy of the Neural Correlate Society; middle middle photograph courtesy of D.M. Barron (oxygengroup); lower middle photograph by P. Opaska; all of these were used with permission; top middle image is a substitute for a configurally identical image that we do not have permission to reproduce). (**b**) Quantification of looking behavior for four control (red) and three face-deprived (green) monkeys from 90 d to 1 year of age. Large black-outlined symbols show means for each monkey. (**c**) Longitudinal looking behavior for four control monkeys from 2 d to >1 year of age at regions containing faces (filled symbols) or at regions containing hands (open symbols). Each symbol represents the percent average looking time at hand or face regions, minus the percent of the entire image covered by the hand or face region, over one viewing session. Yellow bar indicates the range of ages at which control monkeys developed strong stable face patches[20]. (**d**) Same as in **c** for three face-deprived monkeys from 90 d to 383 d of age.

substantially abnormal. Therefore, face deprivation had a dramatic and selective effect on the development of face-selective clusters in IT.

Looking behavior in control and face-deprived monkeys

The lack of face patches in the face-deprived monkeys reveals a major role for visual experience in the formation, or maintenance, of category domains. Furthermore, the foveal bias of face patches and the peripheral bias of scene patches (**Fig. 4**) suggest that where in its visual field the animal experiences these categories may be important in IT domain formation, as has been proposed for humans[14,30]. We therefore asked what young monkeys look at by monitoring their gaze direction when they freely viewed 266 images of natural scenes, lab scenes, monkeys, or familiar humans. In general, all the monkeys tended to look at image regions with high contrast, especially small dark regions and edges (for example, the gaze patterns for the hammer and clothes pins in **Fig. 5a**); but in addition the control monkeys looked disproportionately toward faces, whereas the face-deprived monkeys did not look preferentially at faces and instead looked more often at regions containing hands. **Figure 5a** illustrates the differential looking behavior between control and face-deprived monkeys for nine of the images used in the viewing study. Because there were no systematic differences between control and face-deprived monkeys in where they looked

when viewing images that did not contain hands or faces (for example, the hammer or the clothes pins), we narrowed our analysis to the 19 images in the viewing set that contained prominent faces and hands. **Figure 5** shows the difference in viewing behavior between control and face-deprived monkeys by plotting the average looking time at regions containing faces or regions containing hands for these 19 images (see **Fig. 5a** for examples of regions used). The scatter plot shows the strong tendency of the control monkeys to look disproportionately at faces and of the face-deprived monkeys to look less often at faces and more often at hands. Across viewing sessions, all four control monkeys looked significantly more at faces than at hands, and all three face-deprived monkeys looked significantly more at hands than at faces (two-tailed t-test; controls: B3, $t(20) = 5.2$, $P = 4 \times 10^{-5}$; B4, $t(11) = 10.3$, $P = 5.5 \times 10^{-7}$; B5, $t(13) = 24$, $P = 4 \times 10^{-12}$; B8, $t(17) = 9.6$, $P = 3 \times 10^{-8}$; face-deprived: B6, $t(10) = -8.4$, $P = 7 \times 10^{-6}$; B9, $t(21) = -6.5$, $P = 2 \times 10^{-6}$; B10, $t(12) = -13.6$, $P = 1 \times 10^{-8}$). Although our sample size was too small for robust group-level comparisons, fixed-effects analyses converged with the within-subject analyses ("Group-level fixed-effect analyses" subsection in the Online Methods). The failure of the face-deprived monkeys to look selectively at faces indicates that faces are not inherently interesting or visually salient, so we conclude that the face looking behavior of control monkeys reflected learning from

reinforcement they had received during development rather than an innate tendency to look at faces. Plotting fixation times to face- or hand-containing areas as a function of age (**Fig. 5c,d**) reveals that differential looking behavior, most notably face looking in control monkeys, emerged very early in development, prior to the establishment of category-selective domains, which become detectable by functional MRI (fMRI) only by 150–200 d of age[20]. The face-deprived monkeys' preference for looking at hands in the 19 viewing images need not imply that they normally fixated on their hands all day, but rather that they recognized and attended to hands in these images because they had already learned that hands are the most interesting, animate, or important things in their daily environment.

DISCUSSION

We asked whether face experience is necessary for the development of the face patch system. Monkeys raised without exposure to faces did not develop normal face patches, but did develop domains for scenes, bodies, and hands, all of which they had had extensive experience with. Furthermore, the large-scale retinotopic organization of the entire visual system, including IT, was normal in face-deprived monkeys. Thus, the neurological deficits in response to this abnormal early experience were specific to the never-seen category. These results highlight the malleability of IT cortex early in life and the importance of early visual experience for normal visual cortical development.

A lack of face patches in face-deprived monkeys indicates that face experience is necessary for the formation (or maintenance) of face domains. Our previous study[13] showing that symbol-selective domains form in monkeys as a consequence of intensive early experience indicates that experience is sufficient for domain formation. That experience is both necessary and sufficient for domain formation is consistent with the hypothesis that a retinotopic proto-organization is modified by viewing behavior to become selectively responsive to different categories in different parts of this retinotopic map. Malach and colleagues proposed that an eccentricity organization could precede and drive, by different viewing tendencies for different image categories, the categorical organization of IT[14,15,30]. We recently found that a hierarchical, retinotopic organization is indeed present throughout the entire visual system, including IT, at birth, and therefore could constitute a proto-organization for the development of experience-dependent specializations[18]. Here, we further asked whether early viewing behavior acting on a retinotopic proto-map could produce the stereotyped locations of category domains. We found that control monkeys looked disproportionately at faces, even very early in development, before the emergence of face patches[20] (**Fig. 5c**). A tendency to fixate on faces could contribute to the formation of face domains in foveally biased parts of IT, without requiring any prior categorical bias. The failure to form face patches in the absence of face experience is also a strong prediction of this retinotopic proto-map model. Consistent with this hypothesis, cortical responses to face or body parts are selective for typically experienced configurations[31–33], faces are optimally recognized in an upright, intact configuration[8,9], and experience shapes face-selectivity during infancy and childhood[34–36], all of which corroborate a role for long-term natural experience in generating cortical domains.

A critic could argue that, alternatively, a lack of face patches in face-deprived monkeys could be explained by withering of an innate face domain. The literature in favor of such an innate categorical organization is extensive; however, the most compelling evidence would be finding category-selective domains at birth or a genetic marker for these domains, neither of which have been reported. Face-versus-scene selectivity can be detected (in the same locations that are face selective in adults) in human infants by 5–6 months of age[37] and in macaques as young as 1 month of age[20], but these early 'face' domains are not selective for faces *per se*, as they respond equally well to faces and objects. This early faces>scenes selectivity has been interpreted as evidence for immature innate domains[37] or as eccentricity-based low-level shape selectivity[20], but the absence of face patches in face-deprived monkeys favors the latter interpretation. Our results limit how strong an innate 'category' bias can be; furthermore, the earliest organization cannot be categorical alone, given that a robust retinotopic organization is present in IT at birth in monkeys[18]. Moreover, an innate retinotopic organization carries with it an organization for receptive-field size, and therefore a bias for features such as curvature[13,38] and scale. Thus, the retinotopy model could account for very early selectivity for faces versus scenes, and it predicts a lack of face patches after face deprivation, whereas the category model is undermined by these findings, and by the finding of an innate retinotopic organization[18], to an extent that makes the category model essentially unfalsifiable.

The retinotopic model does require early category-selective looking behavior, but our finding that face-deprived monkeys do not look preferentially at faces as early as 90 d of age indicates that face looking is also unlikely to be innate; rather it must be learned. An innate face recognition system has been proposed to account for infants' tracking faces or face-like patterns[3] or for imitating facial gestures[39,40]; however, other studies have claimed that infants' face looking is based on nonspecific low-level features[7,41] and that newborns do not actually imitate facial gestures[42]. The failure of face-deprived monkeys to look preferentially at faces supports the view that face looking by infants is not innate but is a consequence of low-level perceptual biases and behavioral reinforcement. We have shown that there is an innate retinotopic organization[18], which carries with it a bias for scale and curvature[13,38] in the parts of IT that will become face selective. That, plus a tendency to attend to movement or animacy[43], and the consistent reinforcing value of faces in the infant's environment, could all contribute to preferential face looking behavior, without requiring any innate face-specific mechanisms. Furthermore, a prior study on face-deprived monkeys supports a learned, rather than an innate, basis for face viewing behavior—Sugita's study on face-deprived monkeys[44] has been interpreted as showing an innate bias for looking at faces[2] and for face-discrimination abilities[1,2,45]. However, his finding was not that face-deprived monkeys show significant face looking behavior or face discrimination, but rather that significant differences in face looking and discrimination appear only after face experience. This study is thus consistent with our proposed model in that it does not prove innate face looking or discrimination but does show that early experience shapes preferential looking. A critic nonetheless argues that a lack of preferential face looking by face-deprived monkeys in both our study and Sugita's is consistent with an 'innate face looking behavior that requires the experience of faces to be maintained'. However, as for the innateness of face domains, a face-looking predisposition that requires face experience is a weak innate predisposition and difficult to distinguish from learned behavior.

We propose that IT domains develop as follows: very early in development, reinforcement affects how infants interact with their environment, including what they look at[46]. Looking behavior and an eccentricity-based shape gradient both influence where, on an innate retinotopic proto-map[18], neuronal activity for different image categories predominates. Synapses are retained or strengthened by neuronal activity[47], and local interconnectivity[48] and competition[49] favor clustered retention or strengthening of inputs responsive to similar, or co-occurring, features. This model is parsimonious, and it would mean that the development of IT involves the same kind of activity-dependent,

competitive, self-organizing rules that generate in V1 at birth a precise retinotopic map organized into orientation pinwheels[50].

METHODS

Methods, including statements of data availability and any associated accession codes and references, are available in the online version of the paper.

Note: Any Supplementary Information and Source Data files are available in the online version of the paper.

AUTHOR CONTRIBUTIONS

All authors scanned and reared the monkeys; P.F.S. trained the monkeys; M.S.L., M.J.A., and P.F.S. analyzed the data; and M.S.L. wrote the paper.

COMPETING FINANCIAL INTERESTS

The authors declare no competing financial interests.

Reprints and permissions information is available online at http://www.nature.com/reprints/index.html. Publisher's note: Springer Nature remains neutral with regard to jurisdictional claims in published maps and institutional affiliations.

1. McKone, E., Crookes, K., Jeffery, L. & Dilks, D.D. A critical review of the development of face recognition: experience is less important than previously believed. *Cogn. Neuropsychol.* **29**, 174–212 (2012).
2. McKone, E., Crookes, K. & Kanwisher, N. in *The Cognitive Neurosciences* 4th edn. (ed. Gazzaniga, M.) 467–482 (MIT Press, 2009).
3. Goren, C.C., Sarty, M. & Wu, P.Y. Visual following and pattern discrimination of face-like stimuli by newborn infants. *Pediatrics* **56**, 544–549 (1975).
4. Johnson, M.H., Dziurawiec, S., Ellis, H. & Morton, J. Newborns' preferential tracking of face-like stimuli and its subsequent decline. *Cognition* **40**, 1–19 (1991).
5. Mendelson, M.J., Haith, M.M. & Goldman-Rakic, P.S. Face scanning and responsiveness to social cues in infant rhesus monkeys. *Dev. Psychol.* **18**, 222–228 (1982).
6. Cassia, V.M., Turati, C. & Simion, F. Can a nonspecific bias toward top-heavy patterns explain newborns' face preference? *Psychol. Sci.* **15**, 379–383 (2004).
7. Turati, C., Simion, F., Milani, I. & Umiltà, C. Newborns' preference for faces: what is crucial? *Dev. Psychol.* **38**, 875–882 (2002).
8. Tanaka, J.W. & Farah, M.J. Parts and wholes in face recognition. *Q. J. Exp. Psychol. A* **46**, 225–245 (1993).
9. Young, A.W., Hellawell, D. & Hay, D.C. Configurational information in face perception. *Perception* **16**, 747–759 (1987).
10. Stryker, M.P. *et al.* in *Neurobiology of Neocortex* (eds. Rakic, P. & Singer, W.) 115–136 (Wiley, 1988).
11. Cohen, L. & Dehaene, S. Specialization within the ventral stream: the case for the visual word form area. *Neuroimage* **22**, 466–476 (2004).
12. Aguirre, G.K., Zarahn, E. & D'Esposito, M. An area within human ventral cortex sensitive to 'building' stimuli: evidence and implications. *Neuron* **21**, 373–383 (1998).
13. Srihasam, K., Vincent, J.L. & Livingstone, M.S. Novel domain formation reveals proto-architecture in inferotemporal cortex. *Nat. Neurosci.* **17**, 1776–1783 (2014).
14. Levy, I., Hasson, U., Avidan, G., Hendler, T. & Malach, R. Center–periphery organization of human object areas. *Nat. Neurosci.* **4**, 533–539 (2001).
15. Malach, R., Levy, I. & Hasson, U. The topography of high-order human object areas. *Trends Cogn. Sci.* **6**, 176–184 (2002).
16. Martin, A., Wiggs, C.L., Ungerleider, L.G. & Haxby, J.V. Neural correlates of category-specific knowledge. *Nature* **379**, 649–652 (1996).
17. Ishai, A., Ungerleider, L.G., Martin, A., Schouten, J.L. & Haxby, J.V. Distributed representation of objects in the human ventral visual pathway. *Proc. Natl. Acad. Sci. USA* **96**, 9379–9384 (1999).
18. Arcaro, M.J. & Livingstone, M.S. A hierarchical, retinotopic proto-organization of the primate visual system at birth. *Elife* **6**, e26196 (2017).
19. Harlow, H.F. & Suomi, S.J. Social recovery by isolation-reared monkeys. *Proc. Natl. Acad. Sci. USA* **68**, 1534–1538 (1971).
20. Livingstone, M.S. *et al.* Development of the macaque face-patch system. *Nat. Commun.* **8**, 14897 (2017).
21. Tsao, D.Y., Freiwald, W.A., Knutsen, T.A., Mandeville, J.B. & Tootell, R.B. Faces and objects in macaque cerebral cortex. *Nat. Neurosci.* **6**, 989–995 (2003).
22. Pinsk, M.A., DeSimone, K., Moore, T., Gross, C.G. & Kastner, S. Representations of faces and body parts in macaque temporal cortex: a functional-MRI study. *Proc. Natl. Acad. Sci. USA* **102**, 6996–7001 (2005).
23. Kornblith, S., Cheng, X., Ohayon, S. & Tsao, D.Y. A network for scene processing in the macaque temporal lobe. *Neuron* **79**, 766–781 (2013).
24. Arcaro, M.J. & Livingstone, M.S. Retinotopic organization of scene areas in macaque inferior temporal cortex. *J. Neurosci.* **37**, 7373–7389 (2017).
25. Nasr, S. *et al.* Scene-selective cortical regions in human and nonhuman primates. *J. Neurosci.* **31**, 13771–13785 (2011).
26. Arcaro, M.J., Pinsk, M.A., Li, X. & Kastner, S. Visuotopic organization of macaque posterior parietal cortex: a functional magnetic resonance imaging study. *J. Neurosci.* **31**, 2064–2078 (2011).
27. Janssens, T., Zhu, Q., Popivanov, I.D. & Vanduffel, W. Probabilistic and single-subject retinotopic maps reveal the topographic organization of face patches in the macaque cortex. *J. Neurosci.* **34**, 10156–10167 (2014).
28. Kolster, H. *et al.* Visual field map clusters in macaque extrastriate visual cortex. *J. Neurosci.* **29**, 7031–7039 (2009).
29. Lafer-Sousa, R. & Conway, B.R. Parallel, multistage processing of colors, faces, and shapes in macaque inferior temporal cortex. *Nat. Neurosci.* **16**, 1870–1878 (2013).
30. Hasson, U., Levy, I., Behrmann, M., Hendler, T. & Malach, R. Eccentricity bias as an organizing principle for human high-order object areas. *Neuron* **34**, 479–490 (2002).
31. Chan, A.W., Kravitz, D.J., Truong, S., Arizpe, J. & Baker, C.I. Cortical representations of bodies and faces are strongest in commonly experienced configurations. *Nat. Neurosci.* **13**, 417–418 (2010).
32. de Haas, B. *et al.* Perception and processing of faces in the human brain is tuned to typical feature locations. *J. Neurosci.* **36**, 9289–9302 (2016).
33. Issa, E.B. & DiCarlo, J.J. Precedence of the eye region in neural processing of faces. *J. Neurosci.* **32**, 16666–16682 (2012).
34. Golarai, G., Liberman, A., Yoon, J.M. & Grill-Spector, K. Differential development of the ventral visual cortex extends through adolescence. *Front. Hum. Neurosci.* **3**, 80 (2010).
35. Natu, V.S. *et al.* Development of neural sensitivity to face identity correlates with perceptual discriminability. *J. Neurosci.* **36**, 10893–10907 (2016).
36. Pascalis, O., de Haan, M. & Nelson, C.A. Is face-processing species-specific during the first year of life? *Science* **296**, 1321–1323 (2002).
37. Deen, B. *et al.* Organization of high-level visual cortex in human infants. *Nat. Commun.* **8**, 13995 (2017).
38. Ponce, C.R., Hartmann, T.S. & Livingstone, M.S. End-stopping predicts curvature tuning along the ventral stream. *J. Neurosci.* **37**, 648–659 (2017).
39. Ferrari, P.F. *et al.* Neonatal imitation in rhesus macaques. *PLoS Biol.* **4**, e302 (2006).
40. Meltzoff, A.N. & Moore, M.K. Newborn infants imitate adult facial gestures. *Child Dev.* **54**, 702–709 (1983).
41. Turati, C., Macchi Cassia, V., Simion, F. & Leo, I. Newborns' face recognition: role of inner and outer facial features. *Child Dev.* **77**, 297–311 (2006).
42. Oostenbroek, J. *et al.* Comprehensive longitudinal study challenges the existence of neonatal imitation in humans. *Curr. Biol.* **26**, 1334–1338 (2016).
43. James, W. *The Principles of Psychology* (H. Holt and Company, 1890).
44. Sugita, Y. Face perception in monkeys reared with no exposure to faces. *Proc. Natl. Acad. Sci. USA* **105**, 394–398 (2008).
45. Kanwisher, N. Functional specificity in the human brain: a window into the functional architecture of the mind. *Proc. Natl. Acad. Sci. USA* **107**, 11163–11170 (2010).
46. Bushnell, I.W.R. Mother's face recognition in newborn infants: learning and memory. *Infant Child Dev.* **10**, 67–74 (2001).
47. Hebb, D.O. *The Organization of Behavior; a Neuropsychological Theory* (Wiley, 1949).
48. Livingstone, M.S. Ocular dominance columns in New World monkeys. *J. Neurosci.* **16**, 2086–2096 (1996).
49. Wiesel, T.N. & Hubel, D.H. Comparison of the effects of unilateral and bilateral eye closure on cortical unit responses in kittens. *J. Neurophysiol.* **28**, 1029–1040 (1965).
50. Blasdel, G., Obermayer, K. & Kiorpes, L. Organization of ocular dominance and orientation columns in the striate cortex of neonatal macaque monkeys. *Vis. Neurosci.* **12**, 589–603 (1995).

ONLINE METHODS

Monkeys. fMRI and viewing-behavior studies were carried out on four control and three face-deprived *Macaca mulatta* monkeys, all born in our laboratory, all with excellent health, normal growth, and normal refraction. The monkeys were housed under a 12-h light and 12-h dark cycle. All procedures conformed to USDA and NIH guidelines and were approved by the Harvard Medical School Institutional Animal Care and Use Committee. The control monkeys (three male and one female) were socially housed in a room with other monkeys. The face-deprived monkeys (one male and two female) were hand-reared by laboratory staff members wearing welders' masks, which prevented the monkeys from seeing the staff member's face. The only exposures the monkeys had to faces of any kind were during the scanning sessions and viewing sessions, which constituted at most 2 h per week, with face exposure being a minor fraction of that. The viewing sessions had some images that contained faces, but these sessions were conducted only after the monkeys were 90 d old, and the scanning with some blocks of face images was started only after subject B6 was 225 d old, B9 was 151 d old, and B10 was 173 d old. For scanning, the monkeys were alert, and their heads were immobilized non-invasively using a foam-padded helmet with a chin strap and a bite bar that delivered juice to reward them for looking at the screen. The monkeys were scanned in a primate chair modified to accommodate small monkeys in such a way that they were positioned semi-upright or in a sphynx position. The monkeys were positioned so they could move their bodies and limbs freely, but their heads were restrained in a forward-looking position by the padded helmet. The monkeys were rewarded with juice for looking at the center of the screen. Gaze direction was monitored using an infrared eye tracker (ISCAN, Burlington, MA).

Stimuli. Visual stimuli were projected onto a screen at the end of the scanner bore, 50 cm from the monkey's eyes. All the images covered 20° of visual field. Faces, hands, and objects were centered on a pink-noise background and subtended a similar maximum dimension of 10°. The face, hand, and body mosaics were on a pink-noise background with faces, hands, or bodies covering the entire 20°, as did the scenes. All images were equated for spatial frequency and luminance using the SHINE toolbox[51]. In some sessions we showed both monkey hands and gloved human hands, and in three sessions we showed blocks of gloved hands instead of monkey hands; activations to images of gloved hands were almost identical to activations to monkey hands (**Fig. 1**). Each scan comprised blocks of each image category, each image was presented for 0.5 s, and block length was 20 s, with 20 s of a neutral gray screen with a fixation spot between image blocks. Blocks and images were presented in a counterbalanced order. In most of the early scan sessions for control monkeys, hands were not included in the image sets because we had not yet discovered how strongly face-deprived monkeys responded to hands. One of the control monkeys, B3, was scanned viewing blocks of hands only once, so this monkey's data are included in figures showing individual scan-session data but not in analyses of across-session statistics. The likeness in the right panel of **Figure 5a** is published with informed consent.

Scanning. Monkeys were scanned in a 3-T Tim Trio scanner with an AC88 gradient insert using four-channel surface coils (custom made by A. Maryam at the Martinos Imaging Center). Each scan session consisted of ten or more functional scans. We used a repetition time (TR) of 2 s, an echo time (TE) of 13 ms, a flip angle (α) of 72°, an iPAT = 2, 1-mm isotropic voxels, and a matrix size of 96 × 96 mm, with 67 contiguous sagittal slices. To enhance contrast[52,53] we injected monocrystalline iron oxide nanoparticles (MION; Feraheme, AMAG Pharmaceuticals, Cambridge, MA) at 12 mg per kg body weight in the saphenous vein just before scanning. MION increases the signal-to-noise and inverts the signal[52]; for the readers' convenience we show the negative signal change as positive in all our plots. By using this contrast agent, we were able to reliably obtain clear visual response signals in V1 for single blocks, so we could use eye position data combined with the V1 signal as a quality control measure, to eliminate blocks or entire scans when the monkey was inattentive or not looking at the stimulus[20] (see "Data analysis" subsection below).

Free-viewing behavior. Only a subset of the 19 images that were used in a larger free-viewing study had clearly visible hands and faces and were used in this analysis. Because we wanted to avoid exposing the face-deprived monkeys to faces early in development, we did not show them any of the face-containing images until the monkeys were >90 d old. For each session, all of which occurred during the animals' normal lights-on period, the images from the larger viewing set were presented in random order for 3 s with 200 ms of a black screen between presentations; the image set was presented repeatedly until the monkey stopped looking at the screen. Images ranged from 18.9° × 18.9° of visual angle to 37.8° × 37.8° of visual angle. Monkeys were seated comfortably in a primate chair with their heads restrained using a padded helmet, as for scanning. Gaze direction of the monkey's left eye was collected at a rate of 60 Hz by an infrared eye tracker (ISCAN, Burlington, MA). The monkey's eye was 40 cm from the screen and the eye-tracker camera. A five-point calibration was used at the start of each session. Gaze data were analyzed using Matlab. Data were smoothed, and fixations identified by an algorithm[54] that identifies epochs when eye velocity was <20°/s but rejects closed-eye epochs. Fixations <100 ms or with s.d. >1° were rejected. Fixations that fell >1° outside the border of the presented image were not included in the analysis. In addition, for the heat maps, fixations longer than 2 s.d. above the mean were not included. Heat maps were summed over multiple sessions for each image, smoothed by a 0.25° Gaussian kernel, and normalized to the maximum.

Phase-encoded retinotopic mapping. Eccentricity and polar angle mapping were performed in monkeys B4, B5, and B6 at >1.5 years old and in monkey B9 at 9 months of age, as described in Arcaro *et al.*[26]. To obtain eccentricity maps, the visual stimulus consisted of an annulus that either expanded or contracted around a central fixation point. The annulus consisted of a colored checkerboard with each check's chromaticity and luminance alternating at the flicker frequency of 4 Hz. The duty cycle of the annulus was 10%; that is, any given point on the screen was within the annulus for only 10% of the time. The annulus swept through the visual field linearly. Each run consisted of seven cycles of 40 s each with 10 s of blank, black backgrounds in between. Blank periods were inserted to temporally separate responses to the foveal and peripheral stimuli. Ten to twelve runs were collected with an equal split in direction. It is more difficult for the monkeys to maintain fixation during the eccentricity mapping than during the category runs, and monkey B10 was not yet good enough at fixating to do eccentricity mapping. The polar angle stimulus consisted of a flickering colored checkerboard wedge that rotated either clockwise or counterclockwise around a central fixation point. The wedge spanned 0.5–10.0° in eccentricity with an arc length of 45° and moved at a rate of 9°/s. Each run consisted of eight cycles of 40 s each. Ten to twelve runs were collected with an equal split in the direction of rotation.

Fourier analysis was used to identify spatially selective voxels from the polar angle and eccentricity stimuli. For each voxel, the amplitude and phase (the temporal delay relative to the stimulus onset) of the harmonic at the stimulus frequency were determined by a Fourier transformation of the mean time series. To correctly match the phase delay of the time series of each voxel to the phase of the wedge-and-ring stimuli and thereby localize the region of the visual field to which the underlying neurons responded best, the response phases were corrected for hemodynamic lag (4 s). The counterclockwise (expanding) runs were then reversed to match the clockwise (contracting) runs, and the average response was calculated for each voxel. An *F*-ratio was calculated by comparing the power of the complex signal at the stimulus frequency to the power of the noise (the power of the complex signal at all other frequencies). Statistical maps were thresholded at $P < 0.0001$ (uncorrected for multiple comparisons). Contiguous clusters of spatially selective voxels were identified throughout cortex in both polar-angle- and eccentricity-mapping experiments. A series of visual field maps were identified in general accordance with previous literature[26–28,55]. These included areas V1, V2, V3, V4, V4A, MT, MST, FST, V4t, V3A, DP, CIP1, CIP2, LIP, OTd, PITd, and PITv. Borders between visual field maps were identified based on reversals in the systematic representation of visual space, particularly with respect to polar angle. Eccentricity representations were evaluated to ensure that phase progressions were essentially orthogonal (nonparallel) to the polar angle phase progression and to differentiate between the MT cluster[28] and surrounding extrastriate visual field maps.

Fixation during scanning. To evaluate whether there were differences in how the two monkey groups looked at the different stimuli, we measured the visual response to each image category for each monkey for each scan session in an ROI that covered the central 6–7° of each hemisphere's V1. In four monkeys—B5 (control), B6 (deprived), B8 (control), and B10 (deprived)—the response in V1

was larger to hands than to faces (two-tailed t-test; B5, $t(5) = -5.9$, $P = 0.002$; B6, $t(17) = -7.8$, $P = 0.0001$; B8, $t(5) = -3.1$, $P = 0.03$; B10, $t(11) = -2.4$, $P = 0.04$), probably because the hands were more retinotopically heterogeneous than the faces. In the other two monkeys—B4 (control) and B9 (deprived)—there was no difference between the V1 response to faces and to hands (two-tailed t-test; B4, $t(5) = -2.0$, $P = 0.1$; B9, $t(17) = 0.3$, $P = 0.74$). To look for group-level effects, we performed an analysis of variance (ANOVA) on the means across sessions with monkey as the random effects factor (including the single session for B3). There were no main effects of stimulus (V1 response to faces versus hands; $F(1,21) = 1.97$, $P = 1.7$; monkey group $F(1,21) = 1.43$, $P = 0.24$; or hemisphere $F(1,21) = 0.01$, $P = 0.93$; and no interaction, $F(1,21) < 0.42$, $P > 0.52$). The similarity between control and face-deprived monkeys in V1 response magnitude to hands and faces indicated that there were no differences in fixation behavior during scanning that could explain the large differences between control and face-deprived monkeys in face-selective activations in IT.

We included in our analyses only scans in which the monkeys looked at the screen for more than 80% of the scan. **Supplementary Figure 2** shows the percent of time for each monkey for each scan session for each image category separately for which the monkeys fixated within 5° of the screen center, which was the average area covered by the images. Although fixation performance was slightly worse for deprived monkeys in some scan sessions, there was no systematic difference between categories in the percent time the monkeys' gaze was <5° from fixation (ANOVA; no main effect of monkey group; no main effect of image category and no interaction; $F(1,8) < 1.2$, $P > 0.3$). Furthermore, there was no difference between groups in fixation quality for faces versus other categories, and the data were sufficient to reveal stereotyped hand patches and object patches in every individual scan session (**Fig. 1**). Therefore, it is unlikely that differences in face-selective activity between face-deprived and control monkeys can be attributed to viewing behavior during scanning. The only other potential artifact we could think of would be that the face-deprived monkeys might not have attended to faces as much as the control monkeys did. Such effects of attention should be apparent in the magnitudes of the V1 response[56–58], though certainly attentional modulation could be larger in extrastriate areas[58]. However, there were no differences in V1 activity between groups, indicating that a relative lack of attention cannot explain the lack of face patches in face-deprived monkeys. Furthermore, robust face selectivity has been reported repeatedly in both humans and in monkeys during passive viewing[59], and even in anesthetized monkeys[60]; therefore, a dramatic lack of face responsiveness in our face-deprived monkeys could not be due entirely to differences between groups in attending to faces.

Data analysis. Functional scan data were analyzed using AFNI[61] and Matlab (Mathworks, Natick, MA). Each scan session for each monkey was analyzed separately. Potential 'spike' artifacts were removed using AFNI's 3dDespike. All images from each scan session were then motion-corrected and aligned to a single reference time point for that session first by a six-parameter linear registration in AFNI and then by a nonlinear registration using JIP (written by J. Mandeville, and which accounted for slight changes in brain shape that naturally emerge over the course of a scan session from changes in the distortion field). Scans with movements >0.8 mm were not included in any further analysis. Data were spatially smoothed with a 2-mm full-width at half-maximum kernel to increase the signal-to-noise while preserving spatial specificity. Each scan was normalized to its mean. For each scan, signal quality was assessed within an ROI that encompassed the entire opercular surface of visual area V1 (which covered the central 6–7° of visual field, as confirmed by retinotopic mapping at a later age). Square-wave functions matching the time course of the experimental design were convolved with a MION function[52]. Pearson correlation coefficients were calculated between the response functions and the average V1 response. We used both gaze direction data and average V1 responses to evaluate data quality. We deleted entire scans if the monkey was asleep or was not looking at the screen for at least 80% of the scan, and we censored individual blocks if the V1 response did not fit the MION hemodynamic response convolved with the stimulus time course with a correlation coefficient >0.5. When individual blocks were censored, conditions were rebalanced by censoring blocks from other stimulus conditions starting with the last scan, which typically had the poorest data quality and largest animal movement. Notably, only V1 responses were used for block evaluation.

This scan and block selection was necessary for quality control in these young monkeys, and inclusion of bad scans would have given a false perspective on the responses in each session. Each session was always analyzed first using the entire data set after motion censoring, and this always resulted in noisier, more variable maps and never revealed stronger selectivity for one category versus another than the maps made using only accepted scans and blocks. For **Supplementary Figure 2**, eye-tracking data from each session were averaged over each stimulus-on block type for the graph, and, for the heat maps, smoothed with a 0.5° Gaussian kernel, and normalized to the maximum.

A multiple regression analysis (AFNI's 3dDeconvolve[61]) in the framework of a general linear model[62] was then performed for each scan session separately. Each stimulus condition was modeled with a MION-based hemodynamic response function[52]. Additional regressors that accounted for variance due to baseline shifts between time series, linear drifts, and head motion parameter estimates were also included in the regression model. Due to the time course normalization step, resulting beta coefficients were scaled to reflect the percent signal change. Brain regions that responded more strongly to one image category than to another were identified by contrasting presentation blocks of each image category. Maps of beta coefficients were clustered (>5 adjacent voxels) and thresholded at $P < 0.01$ (FDR-corrected).

Each scan session had enough power to detect category-selective activity. In control monkeys, face patches identified in scan sessions with as few as seven of each block-type repetitions were virtually identical in location and extent to face patches identified in scan sessions with 27 repetitions. In contrast, in face-deprived monkeys, face patches were undetected even in sessions with as many as 33 repetitions of each block type. Although scan sessions for face and object stimuli covered equivalent age ranges for face-deprived and control monkeys, we did not start using hand stimuli in the (older) control monkeys until after we realized that the face-deprived monkeys had such strong hand patches. Given the consistency in location of face and hand patches across sessions (**Figs. 1** and **2**), and the consistency of face domains in control monkeys once they appear during development[20], it is probably safe to assume the hand patches at earlier ages in the control monkeys were similar to these maps.

Conjunction analysis. A conjunction analysis was performed across sessions to evaluate the consistency of faces>objects and hands>objects beta maps in each monkey. Sessions were registered to the F99 standard macaque template[63] in each monkey and collapsed across hemispheres, and beta contrast maps were binarized at a threshold of $P < 0.01$ (FDR-corrected). The proportion of sessions for which each voxel was significantly more activated by faces>objects or by hands>objects were calculated for the three control monkeys and three face-deprived monkeys with multi-session data.

Regions of interest (ROIs). Several ROIs were used to quantify the imaging data. (i) A V1 ROI was drawn on the anatomy of each monkey to cover the entire opercular surface of V1; we confirmed with retinotopic mapping in each monkey (except B10) that this region encompassed the central 6–7° of visual field. (ii) An STS-lower-lip ROI was drawn on the F99 standard macaque brain[63]. This ROI included the entire lower bank and lip of the STS, from its anterior tip back to the prelunate gyrus and MT and V4 borders (as identified by retinotopic mapping) posteriorly. Although the ROI was not constrained by functional data, it was chosen to optimally sample face-selective cortex in control monkeys. The statistics from each scan session were then aligned to the F99 brain, and the number of voxels (mm³) responsive to faces>objects or to hands>objects at $P < 0.01$ (FDR-corrected) were calculated. (iii) The OTS ROI was similarly drawn on the F99 brain to include the OTS and its lower lip, statistics from each scan session were then aligned to the F99 brain, and the number of voxels responsive to bodies>scenes or to scenes>bodies at $P < 0.01$ (FDR-corrected) were calculated. (iv) CIT and AIT ROIs that spanned the lower LIP of the STS, through the fundus and the upper bank were drawn on the F99 brain based on the average location of middle and anterior face and hand patches. We drew these ROIs such that they maximally sampled face patches in control monkeys and hand patches in all monkeys to compare the relative mediolateral locations of face and hand responsiveness with respect to the anatomical landmarks, the banks and fundus of the STS. In each ROI, the shortest cortical distance was calculated between each data point and the crown of the lower lip of the STS. Data were then sorted into 1-mm

bins based on distance from the crown, and average face>object and hand>object beta contrasts were plotted for each bin. (v) Face and hand ROIs were calculated from conjunction maps of faces>objects and hands>objects (thresholded at $P < 0.01$, FDR-corrected), respectively, and an overlap of >40% across scans was set to determine each ROI. The ventral scene ROIs were determined for each monkey based on single-session scenes>bodies contrast maps (thresholded at $P < 0.01$, FDR-corrected).

Group-level fixed-effects analyses. *Face versus hand patches*. To compare face and hand patch sizes between normal and face-deprived monkeys, we performed a three-way ANOVA on the means across sessions (including the single session for B3), with monkey as the random effects factor. Given the small sample size in each group, hemispheres were treated as separate data points, and hemisphere was included as a factor in the analysis. There was a difference in the number of significant ($P < 0.01$, FDR-corrected) category-selective voxels (faces>objects or hands>objects), as well as an interaction with monkey group (control versus face-deprived) (ANOVA, main effect of category, $F(1,21) = 12.56$, $P = 0.002$; interaction between category and monkey group, $F(1,21) = 34.0$, $P = 0.0001$; no main effects of monkey group or hemisphere, and no other interactions, $F(1,21) < 0.58$, $P > 0.45$). Because there was a main effect of category and an interaction with monkey group, we performed *post hoc* comparisons. The average number of face-selective voxels in the STS ROI was smaller in the face-deprived group than in controls (two-tailed unpaired *t*-test averaged over sessions, not hemispheres; $t(12) = -7.6$, $P = 6 \times 10^{-6}$). There was no significant difference in the average number of hand-selective voxels (two-tailed unpaired *t*-test; $t(12) = 1.5$, $P = 0.14$). Although we used a typical number of subjects for a monkey fMRI study, the across-monkey statistics necessarily involved a small sample size. Nevertheless, the results were robust for both across-monkey comparisons, as well as within-animal comparisons, for which we had a much larger sample size.

Body versus scene patches. Across all monkeys (averaged across sessions for B4 and B5) the STS ROI had more significant bodies>scenes voxels, and the OTS had more scenes>bodies voxels (ANOVA; main effect of ROI; $F(1,33) = 5.89$, $P = 0.02$; no main effect of monkey group $F(1,33) = 0.11$; $P = 0.74$, or hemisphere $F(1,33) = 0.01$; $P = 0.95$, and no interaction $F(1,33) < 0.57$; $P > 0.46$). *Post hoc* *t*-tests showed that both control and face-deprived monkeys had more significant body-selective voxels than scene voxels in the STS (two-tailed paired *t*-test; controls, $t(3) = 11.3$, $P = 0.002$; deprived, $t(5) = 3.1$, $P = 0.05$) and that both control and face-deprived monkeys had more significant scene-selective voxels than body voxels in the OTS (two-tailed paired *t*-test; controls, $t(3) = -14.7$, $P = 0.0007$; deprived, $t(5) = -8.2$, $P = 0.0004$). There was no significant difference for either ROI between controls and face-deprived monkeys in the number of significant body voxels (two-tailed unpaired *t*-test; STS, $t(8) = 1.91$, $P = 0.09$; OTS, $t(80) = 0.06$, $P = 0.95$) or scene voxels (STS, $t(8) = -0.981$, $P = 0.35$; OTS, $t(8) = -1.29$, $P = 0.23$).

Free-viewing behavior. To evaluate looking behavior during free viewing as a function of monkey group, we performed an ANOVA on means across sessions with monkey as the random effects factor. The mean looking time per monkey across sessions (>90 d) showed an interaction between monkey group (control versus deprived) and feature category (faces versus hands) (ANOVA; interaction, $F(1,10) = 43.13$, $P < 0.0001$; no main effects of either monkey group or feature category, $F(1,10) < 1.3$, $P > 0.28$).

Experimental design and statistical analysis. Seven monkeys (four control and three face-deprived) were included in stimulus category and behavior analyses. A subset (two control and two face-deprived) were included in retinotopic mapping analyses. Individual subject and group-level analyses were

performed. Although three or four monkeys per group is a small sample size for group-level analyses, this is a typical group size for nonhuman primate studies, and effects were apparent in each individual monkey. Investigators were not blind to group or subject identity. As described in the 'Data analysis' subsection, category-selectivity maps for individual monkeys were determined via a linear regression analysis and thresholded on the resulting *t*-statistics. To assess the consistency of category responses for individual monkeys across sessions, a conjunction analysis was performed based on individual *t*-statistics maps thresholded at $P < 0.01$ (FDR-corrected). Consistency was further evaluated by comparing beta coefficient contrast maps across scans by Pearson correlation. To compare the size of category-selective regions, paired-sample *t*-tests were conducted in individual monkeys across scan sessions. To evaluate group-level stimulus category selectivity, an ANOVA was conducted on the mean number of category-selective voxels (across sessions). Stimulus category, monkey group, and hemisphere were included as factors in the ANOVA. *Post hoc* *t*-tests were then performed accordingly. Retinotopic maps were measured for individual subjects and group averages. Significance was assessed by an *F*-ratio as described in the "Phase-encoded retinotopic mapping" subsection. To evaluate looking behavior during free viewing in individual monkeys, we performed *t*-tests between the mean looking time for different stimulus categories across viewing sessions. As reported in the "Group-level fixed-effects analyses" subsection, looking behavior at the group level was evaluated by an ANOVA on the mean looking time per monkey across sessions. Stimulus category and monkey group were included as factors.

Data and code availability. Data will be made available upon request. We used publically available image analysis software (AFNI, Freesurfer, JIP) and standard Matlab functions for analysis.

A **Life Sciences Reporting Summary** is available.

51. Willenbockel, V. *et al.* The SHINE toolbox for controlling low-level image properties. *J. Vis.* **10**, 653 (2010).
52. Leite, F.P. *et al.* Repeated fMRI using iron oxide contrast agent in awake, behaving macaques at 3 Tesla. *Neuroimage* **16**, 283–294 (2002).
53. Vanduffel, W. *et al.* Visual-motion processing investigated using contrast agent-enhanced fMRI in awake, behaving monkeys. *Neuron* **32**, 565–577 (2001).
54. Wass, S.V., Smith, T.J. & Johnson, M.H. Parsing eye-tracking data of variable quality to provide accurate fixation-duration estimates in infants and adults. *Behav. Res. Methods* **45**, 229–250 (2013).
55. Kolster, H., Janssens, T., Orban, G.A. & Vanduffel, W. The retinotopic organization of macaque occipitotemporal cortex anterior to V4 and caudoventral to the middle temporal (MT) cluster. *J. Neurosci.* **34**, 10168–10191 (2014).
56. Gandhi, S.P., Heeger, D.J. & Boynton, G.M. Spatial attention affects brain activity in human primary visual cortex. *Proc. Natl. Acad. Sci. USA* **96**, 3314–3319 (1999).
57. Martínez, A. *et al.* Involvement of striate and extrastriate visual cortical areas in spatial attention. *Nat. Neurosci.* **2**, 364–369 (1999).
58. Somers, D.C., Dale, A.M., Seiffert, A.E. & Tootell, R.B. Functional MRI reveals spatially specific attentional modulation in human primary visual cortex. *Proc. Natl. Acad. Sci. USA* **96**, 1663–1668 (1999).
59. Tsao, D.Y., Moeller, S. & Freiwald, W.A. Comparing face patch systems in macaques and humans. *Proc. Natl. Acad. Sci. USA* **105**, 19514–19519 (2008).
60. Logothetis, N.K., Guggenberger, H., Peled, S. & Pauls, J. Functional imaging of the monkey brain. *Nat. Neurosci.* **2**, 555–562 (1999).
61. Cox, R.W. AFNI: software for analysis and visualization of functional magnetic resonance neuroimages. *Comput. Biomed. Res.* **29**, 162–173 (1996).
62. Friston, K.J., Frith, C.D., Turner, R. & Frackowiak, R.S. Characterizing evoked hemodynamics with fMRI. *Neuroimage* **2**, 157–165 (1995).
63. Van Essen, D.C. *et al.* An integrated software suite for surface-based analyses of cerebral cortex. *J. Am. Med. Inform. Assoc.* **8**, 443–459 (2001).

Corresponding Author: Margaret Livingstone

Date: 6/6/2017

Life Sciences Reporting Summary

Nature Research wishes to improve the reproducibility of the work we publish. This form is published with all life science papers and is intended to promote consistency and transparency in reporting. All life sciences submissions use this form; while some list items might not apply to an individual manuscript, all fields must be completed for clarity.

For further information on the points included in this form, see Reporting Life Sciences Research. For further information on Nature Research policies, including our data availability policy, see Authors & Referees and the Editorial Policy Checklist.

▶ Experimental design

1. **Sample size**

   Describe how sample size was determined.

   > every session from 4 control and 3 deprived monkeys. 2-3 monkeys is the typical sample size used in primate fMRI studies, so we met the typical sample size for both groups. Further, we had multiple scan sessions in each animal to assess consistency / stability of results).

2. **Data exclusions**

   Describe any data exclusions.

   > we excluded runs when the animals were asleep or not fixating. We state clearly how runs were evaluated, using V1, not IT.

3. **Replication**

   Describe whether the experimental findings were reliably reproduced.

   > we had multiple scan sessions in each animal to assess consistency / stability of results). We discuss the consistency (i.e., repeatability) of the GLM analyses in individual monkeys in the 3rd paragraph of the Results section.

4. **Randomization**

   Describe how samples/organisms/participants were allocated into experimental groups.

   > Control animals were socially housed; face-deprived monkeys were hand-reared without any experience of faces.

5. **Blinding**

   Describe whether the investigators were blinded to group allocation during data collection and/or analysis.

   > Investigators were not blind.

   Note: all studies involving animals and/or human research participants must disclose whether blinding and randomization were used.

6. **Statistical parameters**

   For all figures and tables that use statistical methods, confirm that the following items are present in relevant figure legends (or the Methods section if additional space is needed).

n/a	Confirmed	
☐	☒	The <u>exact</u> sample size (*n*) for each experimental group/condition, given as a discrete number and unit of measurement (animals, litters, cultures, etc.)
☐	☒	A description of how samples were collected, noting whether measurements were taken from distinct samples or whether the same sample was measured repeatedly.
☐	☒	A statement indicating how many times each experiment was replicated
☐	☒	The statistical test(s) used and whether they are one- or two-sided (note: only common tests should be described solely by name; more complex techniques should be described in the Methods section)
☐	☒	A description of any assumptions or corrections, such as an adjustment for multiple comparisons
☐	☒	The test results (e.g. *p* values) given as exact values whenever possible and with confidence intervals noted
☐	☒	A summary of the descriptive statistics, including central tendency (e.g. median, mean) and variation (e.g. standard deviation, interquartile range)
☐	☒	Clearly defined error bars

   See the web collection on statistics for biologists for further resources and guidance.

▶ Software

Policy information about availability of computer code

7. Software

Describe the software used to analyze the data in this study.

> Functional scan data were analyzed using AFNI62 and Matlab (Mathworks, Natick MA). IMages were aligned using a nonlinear registration using JIP (written by Joseph Mandeville).

For all studies, we encourage code deposition in a community repository (e.g. GitHub). Authors must make computer code available to editors and reviewers upon request. The *Nature Methods* guidance for providing algorithms and software for publication may be useful for any submission.

▶ Materials and reagents

Policy information about availability of materials

8. Materials availability

Indicate whether there are restrictions on availability of unique materials or if these materials are only available for distribution by a for-profit company.

> N/A

9. Antibodies

Describe the antibodies used and how they were validated for use in the system under study (i.e. assay and species).

> N/A

10. Eukaryotic cell lines

a. State the source of each eukaryotic cell line used.

> N/A

b. Describe the method of cell line authentication used.

> *Describe the authentication procedures for each cell line used OR declare that none of the cell lines used have been authenticated OR state that no eukaryotic cell lines were used.*

c. Report whether the cell lines were tested for mycoplasma contamination.

> *Confirm that all cell lines tested negative for mycoplasma contamination OR describe the results of the testing for mycoplasma contamination OR declare that the cell lines were not tested for mycoplasma contamination OR state that no eukaryotic cell lines were used.*

d. If any of the cell lines used in the paper are listed in the database of commonly misidentified cell lines maintained by ICLAC, provide a scientific rationale for their use.

> *Provide a rationale for the use of commonly misidentified cell lines OR state that no commonly misidentified cell lines were used.*

▶ Animals and human research participants

Policy information about studies involving animals; when reporting animal research, follow the ARRIVE guidelines

11. Description of research animals

Provide details on animals and/or animal-derived materials used in the study.

> Functional MRI and viewing behavior studies were carried out on 4 control and 3 face-deprived Macaca mulattas, all born in our laboratory, all with excellent health, normal growth, and normal refraction. Animals were housed under a 12-hour light/dark cycle. All procedures conformed to USDA and NIH guidelines and were approved by the Harvard Medical School Institutional Animal Care and Use Committee. The control monkeys (3 male 1 female) were socially housed in a room with other monkeys. The face-deprived monkeys (1 male 2 female) were hand-reared by laboratory staff wearing welders' masks that prevented the monkey from seeing the staff member's face.

Policy information about studies involving human research participants

12. Description of human research participants

Describe the covariate-relevant population characteristics of the human research participants.

> no human subjects

nature research

Corresponding Author: _____

Date: _____

Reporting Summary for MRI studies

Form fields will expand as needed. Please do not leave fields blank.

▶ Experimental design

1. Describe the experimental design.

   | Block design |

2. Specify the number of blocks, trials or experimental units per session and/or subject, and specify the length of each trial or block (if trials are blocked) and interval between trials.

   | 2-6 block types, 20 second blocks, 20 seconds blank. |

3. Describe how behavioral performance was measured.

   | gaze monitoring and V1 response. |

▶ Acquisition

4. Imaging

   a. Specify the type(s) of imaging.

   | functional |

   b. Specify the field strength (in Tesla).

   | 3T |

   c. Provide the essential sequence imaging parameters.

   | repetition time (TR) of 2 seconds, echo time (TE) of 13ms, flip angle of 72 degrees, iPAT = 2, 1mm isotropic voxels, matrix size 96x96mm, 67 contiguous sagittal slices. |

   d. For diffusion MRI, provide full detail on imaging parameters.

   | *Specify # of directions, b-values, single shell or multi-shell and if cardiac gating was used.* |

5. State area of acquisition

   | whole brain |

▶ Preprocessing

6. Describe the software used for preprocessing.

   | AFNI |

7. Normalization

   a. If data were normalized/standardized, describe the approach(es).

   | Each scan was normalized to its mean. |

   b. Describe the template used for normalization/transformation.

   | Each scan was warped using JIP to the standard F99 macaque atlas. |

8. Describe your procedure for artifact and structured noise removal.

   | Each stimulus condition was modeled with a MION-based hemodynamic response function. Additional regressors that accounted for variance due to baseline shifts between time series, linear drifts, and head motion parameter estimates were also included in the regression model. Due to the timecourse normalization, resulting beta coefficients were scaled to reflect % signal change. |

9. Define your software and/or method and criteria for volume censoring and state the extent of such censoring.

   | Scans with movements greater than 0.8 mm were not included in any further analysis. Data were spatially smoothed with a 2mm FWHM kernel |

▸ Statistical modeling & inference

10. Define your model type and settings.

A multiple regression analysis (AFNI's 3dDeconvolve) in the framework of a general linear model was then performed for each scan session separately. Each stimulus condition was modeled with a MION-based hemodynamic response function.

11. Specify the precise effect tested.

Compared blocks of one type to another.

12. Analysis

a. Specify whether analysis is whole brain or ROI-based.

both

b. If ROI-based, describe how anatomical locations were determined.

anatomical criteria on F99 atlas

13. State the statistic type for inference. (See Eklund et al. 2016.)

p<0.01 FDR corrected

14. Describe the type of correction and how it is obtained for multiple comparisons.

FDR

15. Connectivity

a. For functional and/or effective connectivity, report the measures of dependence used and the model details.

E.g. Pearson correlation, partial correlation, mutual information

b. For graph analysis, report the dependent variable and functional connectivity measure.

Weighted graph or binarized graph, specify subject- or group-level, and specify the global and/or node summaries used (e.g. clustering coefficient, efficiency, etc.).

16. For multivariate modeling and predictive analysis, specify independent variables, features extraction and dimension reduction, model, training and evaluation metrics.